



Interactions of fragment ions of tetradecane with solid surfaces



Gikan H. Takaoka*, Mitsuaki Takeuchi, Hiromichi Ryuto, Kousuke Imanaka, Kyohei Hayashi

Photonics and Electronics Science and Engineering Center, Kyoto University, Katsura, Nishikyo-ku, Kyoto 615-8510, Japan

ARTICLE INFO

Article history:

Received 28 June 2013

Received in revised form 12 November 2013

Accepted 21 June 2014

Available online 5 August 2014

Keywords:

Polyatomic ions

Fragment ions

Mass separation

Surface interaction

Irradiation effect

ABSTRACT

Vapors of tetradecane ($C_{14}H_{30}$) were ionized by electron bombardment. The generated fragment ions such as C_3H_7 , C_6H_{13} , and $C_{12}H_{25}$ ions were separated by an $E \times B$ filter (Wien filter) and accelerated toward Si(100) substrates. Thickness measurements showed that thin films were deposited on the Si substrates by C_3H_7 - and C_6H_{13} -ion irradiation, although the Si substrate surface was predominantly sputtered by $C_{12}H_{25}$ ions. Rutherford backscattering spectroscopy showed that the irradiation damage by the fragment-ion beams decreased with the increasing molecular weight of the fragment ions at the same acceleration voltage. Furthermore, Raman spectra as well as X-ray photoelectron spectroscopy measurements showed that DLC films were formed by C_3H_7 - and C_6H_{13} -ion irradiation with the film thickness being larger in case of C_3H_7 . On the contrary, for $C_{12}H_{25}$ -ion irradiation, chemical sputtering occurred by surface reactions of hydrogen and methyl radicals with silicon atoms. The chemical reaction at the irradiated substrate surface could be enhanced by the higher temperatures achieved by the high energy-density irradiation effect of the polyatomic ions.

© 2014 Elsevier B.V. All rights reserved.

1. Introduction

Carbon materials have attracted much interest owing to the large variety of material properties associated with its polymorphism in form of diamond, graphite, fullerene, nanotubes, and graphene. For example, graphene, which is a single sheet of graphite, exhibits unique electron-transport and optical properties [1,2]. Graphene has had a major impact on fundamental research in the field of nanomaterials and provided an excellent platform for exploring novel material properties and enhancing material performance [3]. Furthermore, other carbon materials including graphene exhibit exceptional properties such as extremely high melting points, high hardness, high wear, high chemical inertness, and excellent biocompatibility. For example, fullerenes and nanotubes, which form a curved structure of carbon atoms, tolerate high strain without collapsing. They are excellent candidates for advanced applications in electronics and photonics. In recent years, these carbon materials have been produced by using various kinds of material processing techniques [4–8].

Ion-beam technology is one example of ion-assisted material processing, and it has recently attracted much interest owing to the controllability and variety of applicable ion beams. For example, various kinds of ion beams such as atomic, molecular, and cluster-ion beams are available and widely used in scientific

and technological fields [9–12]. Among these ion beams, a polyatomic molecular ion beam exhibits unique features; one of which is the fact that it can transfer energy and mass, as well as fragment radicals, toward solid surfaces. These fragment radicals play an important role in chemical erosion and sputtering of solid surfaces. Moreover, the impact of polyatomic ions on solid surfaces exhibits unique irradiation effects such as high-density, multiple-collision, and low-energy irradiation effects [13–16]. For example, the high energy-density irradiation effect enhances the surface temperature of the impact region [17,18], which in turn enhances the chemical reaction rates occurring at the surface. Based on these features, polyatomic ion beams can be applied to surface processes such as deposition, etching, shallow implantation, and mixing processes by adjusting the incident energy of the molecular and fragment ions.

Furthermore, concerning polyatomic-molecular-ion irradiation, the critical size is an important factor in the collision process, as it is defined by the number of atoms forming a polyatomic molecular ion and its impact changes from binary to multiple collisions. The analysis of the critical size has attracted much attention from a scientific point of view. In this paper, we focus on tetradecane ($C_{14}H_{30}$) used as polyatomic molecule. In order to clarify the critical size, we produce various kinds of fragments such as C_3H_7 , C_6H_{13} , and $C_{12}H_{25}$ ions. In addition, we investigate the interactions of these fragment ions with Si(100) substrates. Furthermore, carbon-material processing based on ion-beam mixing, deposition, and sputtering is demonstrated using these fragment-ion beams.

* Corresponding author.

2. Experiment

The details of the polyatomic-ion-beam system were described elsewhere [19,20]. Vapors of liquid materials such as normal tetradecane ($C_{14}H_{30}$) were ejected into a vacuum chamber and entered the ionizer. The vapor pressure was maintained at 1.0×10^{-4} Torr. In the ionizer, the vapors were ionized by electron bombardment. Electrons were emitted from a tungsten filament and accelerated by a voltage applied between the filament and the cylindrical anode. The diameter of the cylindrical anode was 20 mm. In order to enhance the ionization efficiency, a mirror-type magnetic field was employed by using a pair of samarium-cobalt permanent magnets, and the magnetic field along the central axis was simultaneously adjusted to 10 mT. The electron voltage for ionization (V_e) was varied between 0 V and 300 V with a corresponding electron current (I_e) adjusted in the range from 0 mA to 100 mA. Several fragment ions were produced by dissociative ionization and extracted by applying a voltage to an extraction electrode. The extraction voltage (V_{ext}) was adjusted between 0 kV and 5 kV.

The extracted ions were mass-separated by an $E \times B$ filter (Wien filter) in which the ion-beam axis, electric field (E) and magnetic field (B) are all mutually perpendicular. The magnetic field was obtained using a cuboid neodymium (Nd) permanent magnet with a surface size of 50 mm \times 50 mm. The magnetic field measured near the surface was 390 mT. The mass-separated ion beams obtained by adjusting the electric field in the $E \times B$ filter were accelerated toward a Si(100) substrate set on a substrate holder. The acceleration voltage (V_a) was tuned between 1 kV and 10 kV. The fluence to the substrates was determined on the basis of the ion current and was maintained at a constant value of 4.0×10^{16} carbon atoms/cm². When the desired fluence was reached, the shutter was closed to terminate ion irradiation. The background pressure around the substrate was 8.0×10^{-7} Torr, attained by using a turbo molecular pump.

3. Results and discussion

3.1. Ion-beam characteristics

The electron-bombardment method produced many fragment ions consisting of polyatomic molecules. Fig. 1 shows the mass spectrum of tetradecane-ion beams. The extraction voltage (V_{ext}) was 3.0 kV, and the electron voltage for ionization (V_e) was 150 V. Furthermore, the electron current for ionization (I_e) was 25 mA, and the magnetic field was 10 mT. As shown in Fig. 1, $C_nH_{2n+1}^+$ ions ($n = 1-14$) are produced, although the mass resolution is not sufficient to unambiguously identify large-mass fragment ions. The mass number of the highest peak is 57, corresponding to the C_4H_9 ion. The second-highest peak corresponds to the C_3H_7 ion with a mass number of 43. In addition, a small peak of $C_{12}H_{25}$ ions is obtained. Compared with the ion current without applying a

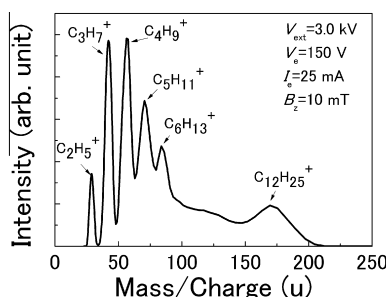


Fig. 1. Mass spectrum of tetradecane-ion beams. The extraction voltage was 3 kV, and the electron voltage for ionization was 150 V.

magnetic field, the extracted ion current was approximately ten times larger and amounted to approximately 55 μ A. Further, the number of fragment ions with a higher mass, such as $C_{12}H_{25}$ ions, increased because the low-energy electrons required for ionization were effectively confined by the magnetic fields.

3.2. Irradiation effect

The irradiation damage by tetradecane-ion beams was investigated by using the Rutherford backscattering spectroscopy (RBS) channeling method. The probe beam was He^+ ion beam with the energy of 2.0 MeV. The scattering angle was 165°. Fig. 2 shows the RBS channeling spectra of the Si(100) surfaces irradiated by C_3H_7 and $C_{12}H_{25}$ ions. The acceleration voltage (V_a) was 6.0 kV. As shown in Fig. 2, the Si surface peak of unirradiated surface is small. It was a few %, which was estimated from the ratio of channeling to random spectra. In addition, the Si surface peak is smaller for $C_{12}H_{25}$ than for C_3H_7 -ion irradiation. This indicates that the irradiation damage by $C_{12}H_{25}$ ions is less pronounced than that induced by C_3H_7 ions. From the area of the Si surface peaks, the number of displaced atoms (N) can be estimated by the equation [21];

$$N = \frac{A - A_0}{H_0} \times \frac{\varepsilon}{[\sigma]} \quad (1)$$

where A and A_0 are the area of the surface peaks for the irradiated and un-irradiated Si(100) surfaces, H_0 is the height of random spectrum of the Si surface peak, ε is the energy per measured channel, and $[\sigma]$ is the stopping cross-section factor. In the RBS channeling measurement, the value of $[\sigma]$ estimated by using the values of parameters such as the incident energy, the scattering angle, and the mass number of probe ion and target atom was 92.6×10^{-15} eVcm². In addition, ε was 1 keV per channel.

Fig. 3 shows the number of displaced atoms of the Si(100) surfaces irradiated by fragment ions such as C_3H_7 , C_6H_{13} , and $C_{12}H_{25}$. The acceleration voltage (V_a) was 6.0 kV. The standard error was estimated to be $\pm 6\%$. As shown in Fig. 3, the number of displaced atoms decreases with the increasing molecular weight of the fragment ions. By assuming that the fragment ions are broken up into atoms after impact onto the surface, the incident energy of a carbon atom in the fragment ion can be estimated. According to a simple estimation, the incident energy of a carbon atom is calculated as the accelerating energy divided by the number of carbon atoms and multiplied by the mass ratio of total carbon atoms to fragment ion. For example, the value is approximately 0.42 keV per carbon atom for $C_{12}H_{25}$ -ion irradiation, which is much less than in the case of C_3H_7 and C_6H_{13} ions. Therefore, the irradiation damage is less for $C_{12}H_{25}$ -ion irradiation owing to the lower irradiation energy.

Fig. 4 shows the number of displaced atoms for the Si(100) surfaces irradiated at an incident energy of approximately 0.42 keV

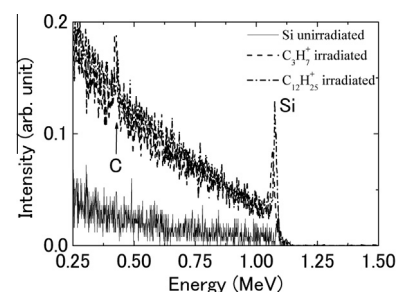


Fig. 2. RBS channeling spectra of the Si(100) surfaces irradiated by C_3H_7 and $C_{12}H_{25}$ ions. The acceleration voltage (V_a) was 6.0 kV, and fluence was 4.0×10^{16} carbon atoms/cm².

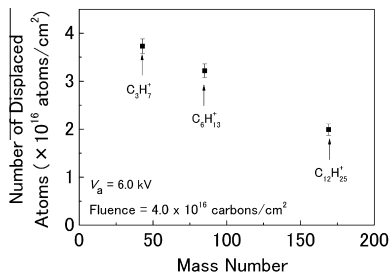


Fig. 3. Number of displaced atoms of the Si(100) surfaces irradiated by fragment ions such as C_3H_7 , C_6H_{13} , and $C_{12}H_{25}$. The acceleration voltage was 6.0 kV, and the fluence was 4.0×10^{16} carbon atoms/cm².

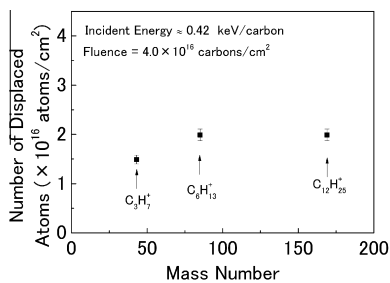


Fig. 4. Number of displaced atoms of the Si(100) surfaces irradiated at an incident energy of approximately 0.42 keV per carbon atom by C_3H_7 , C_6H_{13} , and $C_{12}H_{25}$ ions. Fluence was 4.0×10^{16} carbon atoms/cm².

per carbon atom by C_3H_7 , C_6H_{13} , and $C_{12}H_{25}$ ions. The corresponding acceleration voltages for C_3H_7 , C_6H_{13} , and $C_{12}H_{25}$ ions were 1.5 kV, 3.0 kV, and 6.0 kV, respectively. As shown in the figure, the number of displaced atoms is similar for both C_6H_{13} - and $C_{12}H_{25}$ -ion irradiation because the incident energy per carbon atom in the fragment ions is almost the same, i.e., approximately 0.42 keV. However, the irradiation damage by C_3H_7 is smaller than by C_6H_{13} - and $C_{12}H_{25}$ -ion irradiation. This is due to the formation of carbon layers with a thickness larger than a few nanometers (see Fig. 5). The formed carbon layers stopped the ion irradiation onto the Si surface, which resulted in a decrease in fluence. In addition, taking the effect of hydrogen atoms into account, a hydrogen atom in the fragment ions had an incident energy of approximately 35 eV. In this case, the total incident energy deposited onto the Si surface by the hydrogen atoms is 244 eV and 888 eV for C_3H_7 - and $C_{12}H_{25}$ -ion irradiation, respectively. Therefore, the thermal spike and chemical erosion as well as multiple collisions might be enhanced by the high energy density of $C_{12}H_{25}$ -ion irradiation, which results in an increase of the irradiation damage compared with C_3H_7 -ion irradiation.

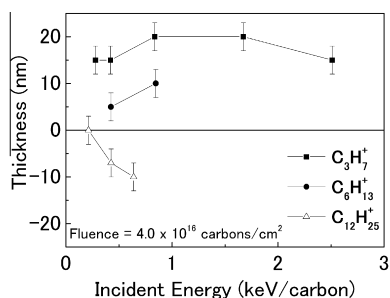


Fig. 5. Thickness of Si(100) surface irradiated at different incident energies per carbon atom by C_3H_7 , C_6H_{13} , and $C_{12}H_{25}$ ions. Fluence was 4.0×10^{16} carbon atoms/cm².

Fig. 5 shows the thickness of Si(100) surfaces irradiated at different incident energies per carbon atom by C_3H_7 , C_6H_{13} , and $C_{12}H_{25}$ ions. The thickness, which is determined by the step difference between the un-irradiated and irradiated surfaces, was measured using the high resolution surface profiler XP-2 (Ambios Technology, Inc.). A positive value was attributed to the film thickness and a negative one to the sputtering depth. The acceleration voltage was adjusted in the range from 0.75 kV to 9 kV. As shown in Fig. 5, the thickness first increases with increasing acceleration voltage for C_3H_7 -ion irradiation; however, it decreases at an acceleration voltage of 9 kV, which corresponds to an incident energy of 2.51 keV per carbon atom and 0.21 keV per hydrogen atom. This indicates that carbon layers are formed by ion-beam mixing and deposition, although the physical sputtering of the Si surfaces occurs at an acceleration voltage of 9.0 kV. In addition, carbon layers are formed for C_6H_{13} -ion irradiation. However, the thickness is smaller than in case of C_3H_7 -ion irradiation. This might be ascribed to chemical sputtering of the Si surfaces by hydrogen atoms included in the C_6H_{13} ions. On the other hand, sputtering predominantly occurs for $C_{12}H_{25}$ -ion irradiation. In addition, the surface roughness measured by an atomic force microscope (AFM) was similar to that of the un-irradiated Si surface, i.e., 0.12 nm. The Si surface irradiated by $C_{12}H_{25}$ ions was flat at an atomic level, even if it was sputtered.

Raman spectra were measured for the Si(100) surfaces irradiated at different acceleration voltages by C_3H_7 and $C_{12}H_{25}$ ions. The acceleration voltage was adjusted between 1.5 kV and 9.0 kV. As shown in Fig. 6, peaks of the D and G band appear at wave numbers of approximately 1300 cm⁻¹ and 1500 cm⁻¹, respectively. These are typical values of diamond-like carbon (DLC) films, although they are weak in the case of $C_{12}H_{25}$ -ion irradiation at an acceleration voltage of 9.0 kV. The peak ratio of the D and G bands, expressed by I_D/I_G , was estimated on the basis of a fitting of the curve areas in Fig. 6, and it is larger for C_3H_7 -ion irradiation than for $C_{12}H_{25}$ -ion irradiation. This indicates that larger amount of SP²-bonded fractions are contained in C_3H_7 -ion-irradiated surfaces [22,23].

Furthermore, the number of hydrogen atoms included in the DLC films can be estimated from the G-band peak intensity (S) with respect to the background signal intensity (N), which is expressed by $N/(S + N)$ [24]. If the ratio is large, more hydrogen atoms are

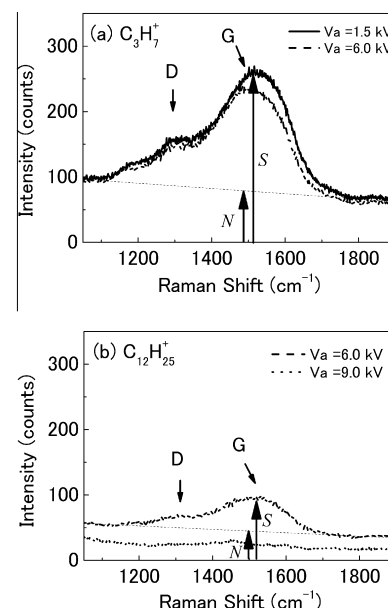


Fig. 6. Raman spectra of Si(100) surfaces irradiated at different acceleration voltages by (a) C_3H_7 and (b) $C_{12}H_{25}$ ions. Fluence was 4.0×10^{16} carbon atoms/cm².

contained in the films. According to this estimation, the DLC thin layer contains more hydrogen atoms if formed by $C_{12}H_{25}$ -ion irradiation than by C_3H_7 -ion irradiation. It should be noted that $C_{12}H_{25}$ ions are dissociated upon surface impact, and some fragments such as methyl radicals are produced. These radicals play another important role in the chemical sputtering process of the Si surfaces as well as in the DLC layer formation. Therefore, DLC layers formed by $C_{12}H_{25}$ -ion beams are thinner and contain more hydrogen atoms.

X-ray photoelectron spectroscopy (XPS) measurements were performed for substrate surfaces after etching. The etching time by argon-ion-beam sputtering was 5 s. Fig. 7 shows the C1s peaks of Si(100) surfaces irradiated by (a) C_3H_7 and (b) $C_{12}H_{25}$ ions. The acceleration voltage was adjusted between 1.5 kV and 9.0 kV. As shown in Fig. 7(a), the C1s peak intensity after C_3H_7 -ion irradiation is similar at the two different acceleration voltages of 1.5 kV and 6.0 kV. Because the depth of implanted carbon atoms is smaller than the XPS detection depth of approximately 5 nm, the total amount of measured carbon atoms corresponds to the fluence. Moreover, as shown in the figure, graphite carbons as well as C–C and C–H bonded carbon atoms are present, although contamination by residual oxygen gas occurs in the deposited DLC films. On the other hand, as shown in Fig. 7(b), the C1s peak intensity after $C_{12}H_{25}$ -ion irradiation is smaller at $V_a = 9.0$ kV compared with that at $V_a = 6.0$ kV. This is ascribed to the enhancement of chemical sputtering, which increases with increasing acceleration voltage. Methyl radicals as well as hydrogen atoms might be involved in the chemical sputtering of the Si substrate surfaces (see Fig. 8). As a result, the number of carbon atoms remaining at the surface decreases with increasing acceleration voltage. Furthermore, another peak corresponding to a Si–C bond appears at a binding energy of 283.3 eV. The chemical reaction between $C_{12}H_{25}$ ions

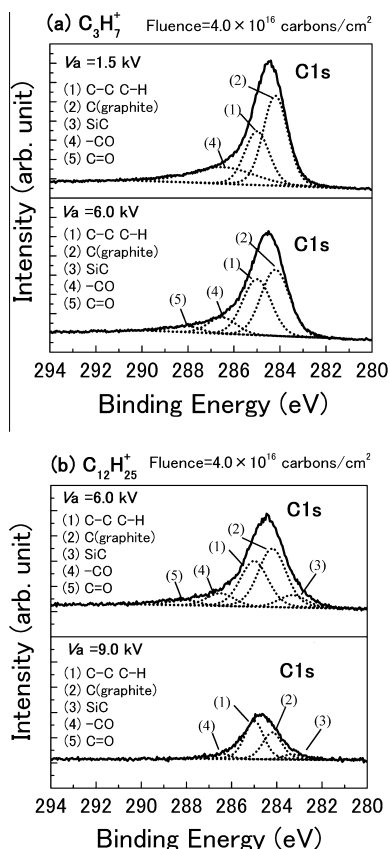


Fig. 7. C1s peaks of Si(100) surfaces irradiated by (a) C_3H_7 and (b) $C_{12}H_{25}$ ions. Fluence was 4.0×10^{16} carbon atoms/cm².

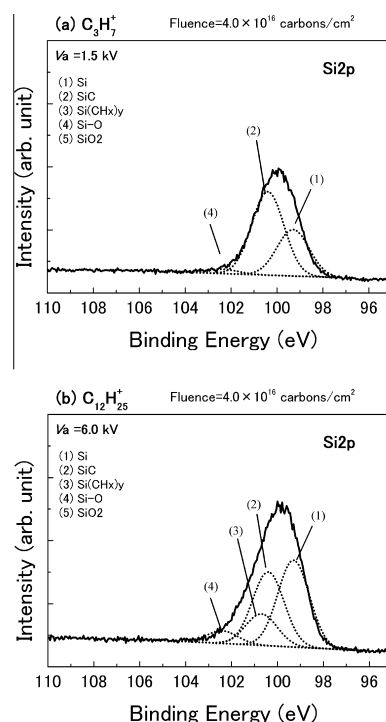


Fig. 8. Si2p peaks of Si(100) surfaces irradiated by (a) C_3H_7 and (b) $C_{12}H_{25}$ ions. Fluence was 4.0×10^{16} carbon atoms/cm².

and Si atoms occurring at the irradiated surface results in the formation of SiC.

In order to confirm the chemical reaction between methyl radicals and Si atoms, the Si2p peak was measured. The etching time was set to 400 s in order to decrease the carbon over-layer thickness. Fig. 8 shows the Si2p peaks of Si(100) surfaces irradiated by (a) C_3H_7 and (b) $C_{12}H_{25}$ ions. The acceleration voltage was adjusted to 1.5 kV and 6.0 kV for C_3H_7 - and $C_{12}H_{25}$ -ion irradiation, respectively. As shown in the figure, the Si2p peak after C_3H_7 -ion irradiation mainly consists of Si and SiC. In addition to these peaks, another peak corresponding to $Si(CH_x)_y$ appears in case of $C_{12}H_{25}$ ion irradiation, which indicates that volatile products, for example $Si(CH_3)_4$, remained at the Si surface after irradiation. With regard to chemical sputtering by $C_{12}H_{25}$ ions, hydrogen atoms as well as methyl radicals play an important role. The number of hydrogen atoms included in a $C_{12}H_{25}$ ion is larger compared with a C_3H_7 ion. Therefore, chemical sputtering occurs in form of evaporation of volatile materials such as silicon hydride and organic silicon compounds. Furthermore, the chemical reaction between silicon atoms and fragment ions increases with increasing surface temperature, which is achieved by the effects of irradiation with a high energy density and multiple collisions of $C_{12}H_{25}$ ions. These effects are neither achieved by the binary collision cascade of atomic ions nor by irradiation with small fragment ions such as C_3H_7 and C_6H_{13} ions. The critical size of the fragment ions could be defined by the number of carbon atoms included, which represent multiple rather than binary collisions. Therefore, a fragment ion with a critical size exists with a stoichiometry between C_6H_{13} and $C_{12}H_{25}$ and involves approximately 10 carbon atoms.

4. Conclusions

Vapors of tetradecane ($C_{14}H_{30}$) were ionized by electron bombardment to produce fragment ions such as C_3H_7 , C_6H_{13} , and $C_{12}H_{25}$. The fragment ions were separated by an $E \times B$ filter and accelerated toward Si(100) substrates. The acceleration voltage was adjusted between 1 kV and 10 kV, and the fluence was

maintained at a constant value of 4.0×10^{16} carbon atoms/cm². Thickness measurements showed that carbon thin films were formed on top of the Si substrates by C₃H₇⁺- and C₆H₁₃⁺-ion irradiation, although the Si substrate surface was sputtered by C₁₂H₂₅⁺-ion irradiation. For C₁₂H₂₅⁺-ion irradiation, chemical sputtering of the Si surfaces by hydrogen atoms as well as methyl radicals might have occurred because the surface temperature of the impact region was enhanced owing to the effect of high-energy-density irradiation by the use of polyatomic ions. Moreover, RBS measurements showed that the damage caused by C₁₂H₂₅⁺-ion irradiation was lower than in the case of C₃H₇⁺- and C₆H₁₃⁺-ion irradiation at the same acceleration voltage, corresponding to a low-energy irradiation effect. Furthermore, according to Raman spectra as well as XPS measurements, DLC films were formed on top of the Si substrates with a larger film thickness for C₃H₇⁺-ion irradiation than for C₆H₁₃⁺-ion irradiation. Thus, polyatomic ions such as the fragment ions of tetradecane exhibit unique irradiation effects that differ in dependence on the mass number corresponding to the number of carbon atoms. In addition, DLC-film formation at room temperature as well as Si surface etching with low irradiation damage was demonstrated using fragment-ion beams by controlling the incident energy.

Acknowledgements

The authors are grateful to the Quantum Science and Engineering Center of Kyoto University for the RBS measurements. In addition, we are grateful to Prof. T. Kuji at Tokai University for Raman spectroscopy measurements.

References

- [1] K.S. Novoselov, A.K. Geim, S.V. Morozov, D. Jiang, Y. Zhang, S.V. Dubonos, I.V. Grigorieva, A.A. Frisov, *Science* 306 (2004) 666.
- [2] A.K. Geim, K.S. Novoselov, *Nat. Mater.* 6 (2007) 183.
- [3] W. Lu, P. Soukiassian, J. Boeckl, *MRS Bull.* 37 (2012) 1119.
- [4] H.W. Kroto, J.R. Heath, S.C. O'Brien, R.F. Curl, R.E. Smalley, *Nature* 318 (1985) 162.
- [5] S. Iijima, *Nature* 354 (1991) 56.
- [6] B. Kitiyanan, W.E. Alvarez, J.H. Harwell, D.E. Resasco, *Chem. Phys. Lett.* 317 (2000) 497.
- [7] J. Ishikawa, *Surf. Coat. Technol.* 65 (1994) 64.
- [8] F.Z. Cui, D.J. Li, *Surf. Coat. Technol.* 131 (2000) 481.
- [9] H. Haberland, *Clusters of Atoms and Molecules*, Springer-Verlag, Berlin, 1994.
- [10] H. Yasumatsu, T. Kondow, *Rep. Prog. Phys.* 66 (2003) 1783.
- [11] D.J. Stokes, L. Roussel, O. Wilhelmi, L.A. Giannuzzi, D.H.W. Hubert, *Mater. Res. Soc. Proc.* 1020 (2007) 15.
- [12] J. Ishikawa, *Rev. Sci. Instrum.* 79 (2008) 02C506.
- [13] K. Goto, J. Matsuo, T. Seki, H. Hinakata, I. Yamada, T. Hisatsugu, *IEDM Tech. Dig.* (1996) 435.
- [14] Z. Herman, *Int. J. Mass Spectrom.* 233 (2004) 361.
- [15] N.G. Rudawski, L.R. Whidden, V. Craciun, K.S. Jones, *J. Electr. Mater.* 38 (2009) 1926.
- [16] G.H. Takaoka, H. Ryuto, M. Takeuchi, *J. Mater. Res.* 27 (2012) 806.
- [17] Z. Insepov, M. Sosnowski, G.H. Takaoka, I. Yamada, *Mater. Res. Soc. Proc.* 316 (1994) 999.
- [18] Z. Insepov, I. Yamada, *Surf. Rev. Lett.* 3 (1996) 1023.
- [19] G.H. Takaoka, M. Takeuchi, H. Ryuto, *Rev. Sci. Instrum.* 81 (2010) 02B302.
- [20] M. Takeuchi, H. Ryuto, G.H. Takaoka, *Proc. of IPAC'10, Kyoto, Japan* (2010) p. 136.
- [21] W.-K. Chu, J.W. Mayer, M.-A. Nocolet, *Backscattering Spectrometry*, Academic Press Inc., New York, 1978, Chap. 5 and 8.
- [22] T. Mikami, H. Nakazawa, M. Kudo, M. Mashita, *Thin Solid Films* 488 (2005) 87.
- [23] A. Ferrari, C. Robertson, *Phys. Rev. B* 61 (2000) 14095.
- [24] K. Miura, M. Nakamura, *J. Surf. Finish. Soc. of Japan* 59 (2008) 51. in Japanese.